

Resistivity and optical conductivity of cuprates within the t - J model

M. M. Zemljic¹ and P. Prelovsek^{1,2,3}¹*J. Stefan Institute, SI-1000 Ljubljana, Slovenia*²*Faculty of Mathematics and Physics, University of Ljubljana, SI-1000 Ljubljana, Slovenia*³*Max-Planck-Institut für Festkörperforschung, D-70569, Germany*

(Received 25 April 2005; published 2 August 2005)

The optical conductivity $\sigma(\omega)$ and the dc resistivity $\rho(T)$ within the extended t - J model on a square lattice, as relevant to high- T_c cuprates, are reinvestigated using the exact-diagonalization method for small systems, improved by performing a twisted boundary condition averaging. The influence of the next-nearest-neighbor hopping t' is also considered. The behavior of results at intermediate doping is consistent with a marginal-Fermi-liquid scenario and in the case of $t'=0$ for $\omega > T$ follows the power law $\sigma \propto \omega^{-\nu}$ with $\nu \sim 0.65$ consistent with experiments. At low doping $c_h < 0.1$ for $T < J$ $\sigma(\omega)$ develops a shoulder at $\omega \sim \omega^*$, consistent with the observed midinfrared peak in experiments, accompanied by a shallow dip for $\omega < \omega^*$. This region is characterized by the resistivity saturation, whereas a more coherent transport appears at $T < T^*$ producing a more pronounced decrease in $\rho(T)$. The behavior of the normalized resistivity $c_h \rho(T)$ is within a factor of 2 quantitatively consistent with experiments in cuprates.

DOI: 10.1103/PhysRevB.72.075108

PACS number(s): 71.27.+a, 72.10.-d, 74.72.-h

I. INTRODUCTION

Since the discovery of high- T_c cuprates, strong correlations among electrons have been considered as the crucial reason for anomalous transport properties in the normal state of these materials. Prominent example is the dc resistivity obeying the well-known linear law, $\rho \propto T$, in the intermediate (optimum) range of hole doping accompanied by an anomalous but universal frequency dependent optical conductivity $\sigma(\omega)$, phenomenologically described via a marginal-Fermi-liquid (MFL) scenario¹ or the quantum-critical behavior.² In the last decade the emphasis has been centered on the experimental investigations of the underdoped regime in various cuprates. The main signatures of this regime are the kink in dc $\rho(T)$ at the crossover scale T^* (Refs. 3 and 4) and the appearance of a broad peak in the infrared region (mid-IR) (Ref. 5) as well as of the pseudogap scale in $\sigma(\omega)$.^{6,7} Recently, it has been established within this regime that the mobility of holes increases with doping concentration.⁸

From the theoretical point of view, it is not an easy task to construct an analytical transport theory for strongly correlated systems, starting from a microscopic model that describes the motion of charge in a weakly or moderately doped antiferromagnetic (AFM) insulator. Even at present such a theory is lacking. However, numerical investigations of the prototype models, in particular of the t - J model, show that $\sigma(\omega)$ and $\rho(T)$ of cuprates can be reasonably accounted for. Application of the finite-temperature Lanczos method (FTLM) (Refs. 9 and 10) to small systems yields results being most reliable in the regime of intermediate doping^{11,12} where also the experimental window $T < 1000$ K can be probed best. In the latter regime, numerical results show an overall agreement with the simple scaling $\sigma(\omega) \propto [1 - \exp(-\omega/T)]/\omega$, with the only scale given by the temperature T .^{10,12}

Recently, several aspects of the conductivity in cuprates have been reopened urging for reconsideration and improve-

ment of theoretical and model results. Detailed experimental studies in the optimally doped cuprate $\text{Bi}_2\text{Sr}_2\text{Ca}_{0.92}\text{Y}_{0.08}\text{Cu}_2\text{O}_{8+\delta}$ (BSCCO) (Ref. 2) reveal for $\omega > T$ the T -independent power-law behavior $\sigma(\omega) \propto \omega^{-\nu}$ with $\nu \sim 0.65$. The authors attribute such a scaling to the vicinity of the quantum-critical point.²

Another question is the existence and value of the resistivity saturation in cuprates at low hole doping.^{13,14} It has been realized that cuprates at high T and low doping show very large resistivity ρ (Refs. 3 and 8) and thus violate the naive Ioffe-Regel condition for metals, which implies a saturation of $\rho(T)$ when the scattering length L_s reaches the intercell distance. On the basis of the t - J model the modified saturation value ρ_{sat} has been derived¹³ and its anomalous large value has been ascribed to the kinetic energy being strongly suppressed due to strong correlations, in particular $\langle H_{\text{kin}} \rangle \propto c_h$ close to half-filling, where $c_h = N_h/N$ is the hole number concentration. From the experimental view, $\text{La}_{2-x}\text{Sr}_x\text{CuO}_4$ (LSCO) serves as a prototype cuprate with a well controlled hole doping $c_h = x$ and stable material properties. Previous and recent results^{3,8} in single-crystal LSCO have revealed signatures of saturation at high $T > T^* \sim 500$ K. Plausibly, the saturation phenomenon is related to the emergence of a T window, where $\sigma(\omega < \omega^*)$ is quite flat or even develops a shallow dip.^{15,16} The latter phenomenon is clearly related to the appearance of a broad mid-IR peak at $\omega \sim \omega^*$ first found at low doping in LSCO (Refs. 5 and 15) and recently also in $\text{YBa}_2\text{Cu}_3\text{O}_y$ (YBCO).¹⁶

Recently, estimates were presented^{13,14} that the t - J model yields substantially smaller resistivity $\rho(T)$ than experiments in LSCO for the regime of low doping. This apparently leads to a conclusion that coupling to additional degrees of freedom, in particular to phonons, might be essential to explain the large resistivity. This aspect is clearly of importance since it is related to the central question, i.e., to what extent the t - J model and strong correlations alone can describe the physics of high- T_c cuprates.

The existence of the mid-IR resonance in $\sigma(\omega)$ is experimentally well established at low doping,^{5,15,16} however the consensus on its origin has not been reached yet. We note that such a peak has been reproduced already in calculations of $\sigma(\omega)$ for a single hole within the t - J model at $T=0$ (Ref. 17) and has been attributed to the string picture of incoherent hole motion leading to the shoulder at $\omega^* \sim 2J$.¹⁸ However, a confirmation of this feature in more realistic $T>0$ calculation was missing so far.

The aim of this paper is to give answers to the above questions via a systematic reinvestigation of $\sigma(\omega)$ and $\rho(T)$ within the extended t - J model, considering also the influence of the next-nearest-neighbor (NNN) hopping t' which has already been invoked in the modeling of hole and electron doped cuprates¹⁹ to possibly reveal the pronounced difference of $\sigma(\omega)$ between both classes of cuprates. Additional hopping parameter t' has been identified to be important for the explanation of spectral properties, e.g., the band dispersion as measured via the angle-resolved photoemission experiments (ARPES).²⁰ Even more, $t' < 0$ could be the essential parameter discriminating various families of hole-doped cuprates (LSCO, BSCCO, etc.),^{21,22} in particular their superconducting transition temperature T_c . Relative to the previous work^{10,11} we are able to study somewhat larger size systems using the FTLM. At the same time we improve the method by introducing averaging over twisted boundary conditions (TBC), described further. The improvement shows up in a more controlled behavior of $\sigma(\omega)$ at low ω , being essential to extract reproducible $\rho(T)$ at lower T . In the intermediate doping we present calculations for systems up to $N=20$ sites to clarify the universal behavior of $\sigma(\omega)$. In the low-doping regime we study systems up to $N=26$ sites allowing us to establish the emergence of a pseudogap scale in $\sigma(\omega)$ as well as the onset of a more coherent transport for $T < T^*$. Our results still remain restricted to $T > 400$ K. Nevertheless, they confirm the qualitative behavior of $\sigma(\omega)$ in cuprates, with the quantitative discrepancy in $\rho(T)$ compared to experiments within a factor of 2 at most.

The paper is organized as follows. In Sec. II the improved FTLM method, employing the TBC averaging, is described. The comparison of results with the usual fixed-boundary condition (BC) method is presented. In Sec. III the optimum doping results for $\sigma(\omega)$ and $\rho(T)$ are presented and discussed in connection with the scaling behavior and experimental results for cuprates. In Sec. IV the low-doping regime is examined, with the emphasis on the emergence of the shoulder corresponding to the mid-IR peak in $\sigma(\omega)$, the resistivity saturation and the onset of a coherent transport for $T < T^*$. Conclusions are given in Sec. V.

II. NUMERICAL METHOD

In the following we study numerically the extended t - J model,

$$H = - \sum_{i,j,s} t_{ij} \tilde{c}_{js}^\dagger \tilde{c}_{is} + J \sum_{\langle ij \rangle} \left(\mathbf{S}_i \cdot \mathbf{S}_j - \frac{1}{4} n_i n_j \right), \quad (1)$$

on a square lattice, whereby we include besides the nearest-neighbor (NN) hopping $t_{ij}=t$ also NNN hopping $t_{ij}=t'$.

Strong correlations among electrons are incorporated via projected operators, e.g., $\tilde{c}_{is}^\dagger = (1 - n_{i,-s}) c_{is}^\dagger$, which do not allow for a double occupancy of sites. The dependence of $\sigma(\omega)$ on t' has already been examined in connection with the difference between the hole-doped and electron-doped cuprates.¹⁹ However, the influence of t' on the dc transport is less evident and has not been studied systematically so far.¹⁰ Plausibly, it is expected that $t' < 0$, being appropriate for hole-doped cuprates, leads to a larger frustration of the AFM spin background and consequently to a larger resistivity. In our study we will test the behavior at three different $t'=0$, $t'=-0.15t$, and $t'=-0.3t$, respectively. We keep everywhere $J=0.3t$ as appropriate for cuprates, as well as we note that $t \sim 0.4$ eV for a direct comparison with experiments.

The main limitation to the validity of numerical results comes from the finite-size effects which begin to dominate results at low $T < T_{fs}$. As a criterion for T_{fs} we use the thermodynamic sum¹⁰

$$\bar{Z}(T) = \text{Tr} \exp[-(H - E_0)/T], \quad (2)$$

calculated in a given system for fixed hole number N_h and the requirement $\bar{Z}(T_{fs}) = Z^* \gg 1$. In the following we use $Z^* \sim 30$.

Finite size effects can be substantially reduced by employing the TBC averaging.^{23,24} In a system with periodic BC the latter is achieved by introducing a uniform vector potential $\vec{\theta}$ modifying the hopping elements $t_{ij} \rightarrow \tilde{t}_{ij} = t_{ij} \exp(i\vec{\theta} \cdot \vec{r}_{ij})$ by a phase factor. We use further N_t different phases $\vec{\theta}$ instead of the usually fixed BC $\theta=0$. For an arbitrary operator A we then perform the usual thermodynamic averaging over N_t different TBC,

$$\langle A \rangle = \frac{\sum_{j=1}^{N_t} \langle A \rangle_j Z_j}{\sum_{j=1}^{N_t} Z_j}, \quad (3)$$

where $\langle A \rangle_j$ and Z_j refer to the canonical FTLM expectation values obtained for each fixed phase $\vec{\theta}$. In order to preserve the translational invariance of the lattice Hamiltonian in 2D we are allowed to study tilted square lattices with N sites where N must be Pythagorean, i.e., $N = n^2 + m^2$. Consequently the first Brillouin zone, where the phases are chosen equidistantly, is a tilted square and N_t is also chosen Pythagorean, so that the phases form a regular square lattice as well. Effectively, such a choice reproduces, e.g., for free fermions the regular (square) lattice of NN_t points in the \mathbf{k} space within the first Brillouin zone.

There are several advantages of the TBC averaging procedure.

(a) In the limit $T \rightarrow 0$ (for large enough N_t) this method reproduces for an arbitrary quantity, e.g., for $\sigma(\omega)$, the result corresponding to the ground state wave function $|\Psi_0(\vec{\theta})\rangle$ with $E_0(\vec{\theta}) = \min$ for a chosen system with N sites and N_h holes.

(b) In a finite (nonintegrable) system, even for $T > 0$, we generally expect the 2D optical conductivity of the form

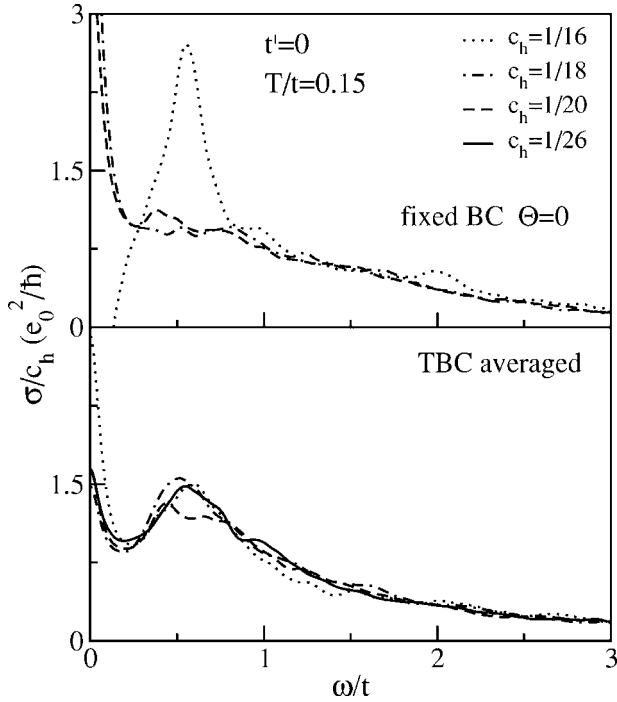


FIG. 1. Dynamical 2D mobility σ/c_h for a single hole $N_h=1$ in different systems $N=16, 18, 20, 26$ evaluated at fixed $T/t=0.15$, (a) for fixed BC $\theta=0$, and (b) with the TBC averaging.

$$\sigma(\omega) = 2\pi D_c \delta(\omega) + \sigma_{reg}(\omega), \quad (4)$$

where

$$D_c = \frac{1}{2N} \langle \tau \rangle - \frac{1}{\pi e_0^2} \int_0^\infty \sigma(\omega) d\omega, \quad (5)$$

D_c is the charge stiffness representing the nondissipative part of conductivity, emerging due to nonscattered coherent charge propagation in a finite system with periodic BC, and $\langle \tau \rangle$ is the kinetic stress tensor or the generalized kinetic energy which in the case of NN hopping on a square lattice reduces to the usual kinetic energy, i.e., $\langle \tau \rangle = -\langle H_{kin} \rangle / 2$.²⁵ Since $D_c(T=0) \propto \partial^2 E_0(\vec{\theta}) / \partial^2 \vec{\theta} |_{E_0(\vec{\theta})=\min} > 0$,²⁶ the TBC averaging leads automatically to $D_c(T \rightarrow 0) > 0$ as appropriate for a metal. Note that previous calculations of $\sigma(\omega)$ at fixed $\theta=0$ (Refs. 10 and 11) generally suffered on a quite system dependent $D_c(T \rightarrow 0)$ which was in many cases even negative.

(c) In general, the TBC averaging reduces finite-size effects, although it cannot completely eliminate them. Results for $\sigma(\omega)$ are thus more size and shape independent. In Fig. 1 we present the comparison of results for a single hole $N_h=1$ in different systems $N=16, 18, 20, 26$, as obtained for a fixed BC $\theta=0$ and when using the TBC averaging. There is a clear difference in the low- ω regime where D_c can be even negative for a fixed BC, while rather consistent results are obtained when applying the improved method. Moreover, the TBC averaged $\sigma(\omega)$ display quite evident and consistent shoulder at $\omega^* \sim 0.5t$, corresponding to the mid-IR peak in

cuprates,^{5,15,16} while this feature is hardly visible for fixed BC spectra.

In the following, we present results using typically $N_l \sim 10$ and $M \sim 140$ Lanczos steps within each symmetry sector of the Hilbert space. Since TBC averaging now also takes the role of random sampling we do not perform any additional sampling over the initial Lanczos wave function within each sector. In each of the available systems $N=18, 20, 26$ we are able to reach $T_{fs} \sim 0.1t$ for the intermediate doping and somewhat higher for low doping. In the analysis of $\sigma(\omega)$ spectra broadening $\epsilon=0.07t$ is used.

III. INTERMEDIATE-OPTIMUM DOPING

One of the most striking facts in cuprates, recognized from the beginning, is the universality of the charge response $\sigma(\omega, T)$ in the vicinity of the optimum doping. Whereas the dc resistivity shows a linear variation $\rho(T) \propto T$, also $\sigma(\omega)$ can be analyzed with an anomalous Drude-type relaxation rate $1/\tau(\omega, T) \propto \omega + \xi T$. The only relevant ω scale seems to be given by T itself, as summarized within the phenomenological MFL scenario.¹ Recent study of optimally doped BSCCO system has revealed, that at low T in a broad range of $T < \omega < 0.5$ eV one can describe results with a power law $\sigma(\omega) \propto \omega^{-\nu}$, whereby $\nu \sim 0.65$.² Still, it is not possible to represent results for $\sigma(\omega, T)$ in the whole (ω, T) range with a single universal function of ω/T as, e.g., required within the quantum-critical-point scenario.²

Numerical results for $\sigma(\omega)$ within the t - J model are most reliable at intermediate doping, since there the lowest T_{fs} can be reached within a fixed system of N sites.¹⁰ In Fig. 2 we present results for a lattice of $N=20$ sites and $N_h=3$ holes, i.e., the hole doping $c_h=N_h/N=0.15$, at various T/t and different $t'/t=0, -0.15, -0.3$. Obtained 2D $\sigma(\omega)$ can serve as a test for the scaling behavior. The optical sum rule,

$$\int_{-\infty}^{\infty} \sigma(\omega) d\omega = \frac{\pi e_0^2}{N} \langle \tau \rangle, \quad (6)$$

requires a fast fall-off of $\sigma(\omega)$ for large $\omega > \omega_c$, hence one can discuss the scaling only for $\omega < \omega_c \sim 2t$.

In Fig. 3 we study $\sigma(\omega)$ for $t'=0$ within the regime $T < \omega < \omega_c$. We see that the fall-off is slower than $\propto 1/\omega$ and is well described with the power law $\sigma \propto \omega^{-\nu}$ with $\nu < 1$. Still, ν seems to depend slightly on t' . The closest fit for $t'=0$ yields $\nu=0.65$ which is in excellent agreement with experiments in BSCCO,² although for the latter cuprates a more appropriate model should be the one with $t' < 0$. For $t' < 0$ our results reveal a decreasing ν . That is, we get for $t'/t=-0.15$ and $t'/t=-0.3$, $\nu=0.5$ and $\nu=0.42$, respectively.

In order to come closer to the understanding of the scaling behavior, we represent $\sigma(\omega)$ in a general form following the Kubo formula:

$$\sigma(\omega) = C(\omega) \frac{1 - e^{-\omega/T}}{\omega}, \quad (7)$$

where $C(\omega)$ is current-current correlation function

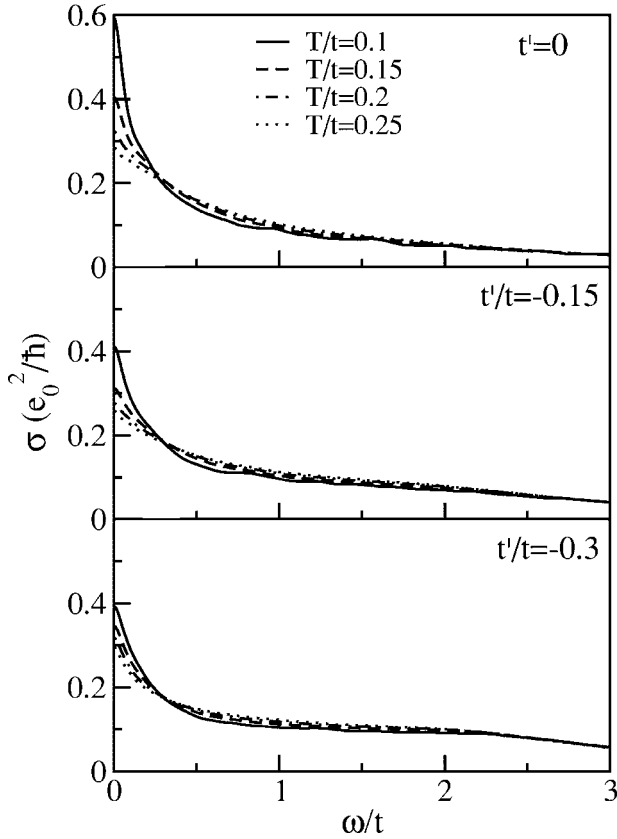


FIG. 2. 2D optical conductivity $\sigma(\omega)$ for the intermediate doping $c_h=3/20$ as calculated for $N=20$ square lattice for different T/t and $t'/t=0, -0.15, -0.3$.

$$C(\omega) = \text{Re} \int_0^\infty dt e^{i\omega t} \langle j(t)j \rangle. \quad (8)$$

It has been observed that the scaling behavior of $\sigma(\omega, T)$ within the t - J model at intermediate doping can be well described up to the cutoff $\omega < \omega_c$ by a parameter-free form of Eq. (7) with $C(\omega) \sim C_0$ where C_0 is T independent. Such a form is clearly a restricted version of the MFL behavior¹ and reproduces both $\rho \propto T$ law and $\sigma(\omega \gg T) \propto 1/\omega$. In view of

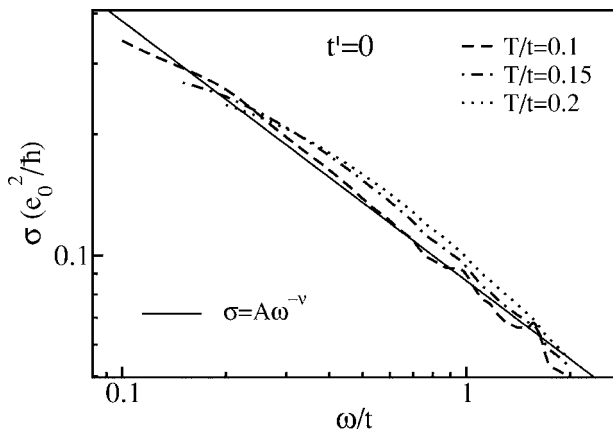


FIG. 3. Log-log plot of σ vs. ω for $c_h=3/20$. Full line represents the closest fit to the power law with $\nu=0.65$ for $T/t=0.1$.

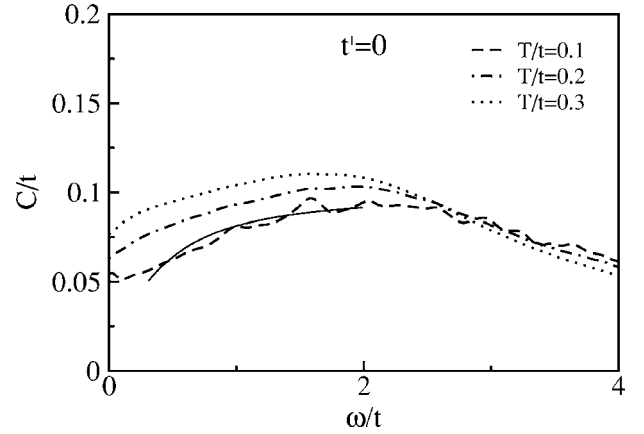


FIG. 4. $C(\omega)$ for intermediate doping $c_h=3/20$ and various T/t . Full line represents the analytical result from Eq. (11) with $\gamma=1.2$, $\xi=\pi$, and $T/t=0.1$.

present improved results presented in Fig. 3 we can analyze the deviation from the simple $C(\omega)=C_0$ form. In Fig. 4 we show $C(\omega)$ for $t'=0$ and various T/t . In this case the spectra are broadened with the factor $\epsilon=0.1t$. The main characteristic is that $C(\omega)$ is an increasing function for $\omega < \omega_c$, consistent with effective $\nu < 1$.

The origin of a very broad range of validity of $\sigma \propto \omega^{-\nu}$ has not become clear yet. Note that $\nu < 1$ requires an increasing $C(\omega)$ which in normal metals is supposed to have a Lorentzian form with a characteristic width determined by a Drude relaxation rate $1/\tau < T$. The interpretation of the anomalous (constant or even increasing) $C(\omega)$ has been proposed by one of the authors.²⁷ By performing a simple decoupling of $C(\omega)$ in terms of the single-electron spectral functions $A(\mathbf{k}, \omega)$ and neglecting the vertex corrections, one gets

$$C(\omega) = \frac{2\pi e_0^2}{N} \sum_{\mathbf{k}} (v_{\mathbf{k}}^\alpha)^2 \int d\omega' \times f(-\omega') f(\omega' - \omega) A(\mathbf{k}, \omega') A(\mathbf{k}, \omega' - \omega), \quad (9)$$

where f is the Fermi function and $v_{\mathbf{k}}^\alpha$ unrenormalized band velocities. We represent $A(\mathbf{k}, \omega)$ for quasiparticles close to the Fermi energy as

$$A(\mathbf{k}, \omega) = \frac{1}{\pi} \frac{Z_{\mathbf{k}} \Gamma_{\mathbf{k}}}{(\omega - \epsilon_{\mathbf{k}})^2 + \Gamma_{\mathbf{k}}^2}, \quad (10)$$

where parameters $Z_{\mathbf{k}}$, $\Gamma_{\mathbf{k}}$, $\epsilon_{\mathbf{k}}$ in general are dependent on T . In order to reproduce the MFL scaling of $\sigma(\omega)$ we must assume the MFL form for the damping, i.e., $\Gamma = \gamma(|\omega| + \xi T)$ as well as neglect the \mathbf{k} dependence of Γ and Z . With these simplifications we arrive at

$$C(\omega) = \bar{C} \int d\omega' f(-\omega') f(\omega' - \omega) \frac{\bar{\Gamma}(\omega, \omega')}{\omega^2 + \bar{\Gamma}(\omega, \omega')^2}, \quad (11)$$

where $\bar{\Gamma}(\omega, \omega') = \Gamma(\omega') + \Gamma(\omega' - \omega)$. It has been noted²⁷ that $C(\omega) \sim C_0$ appears already for $\gamma \sim 0.3$, while for $\gamma > 0.3$ it is an increasing function of ω/T . We should also remind that $\gamma > 0.3$ is consistent with ARPES experiments in BSCCO,

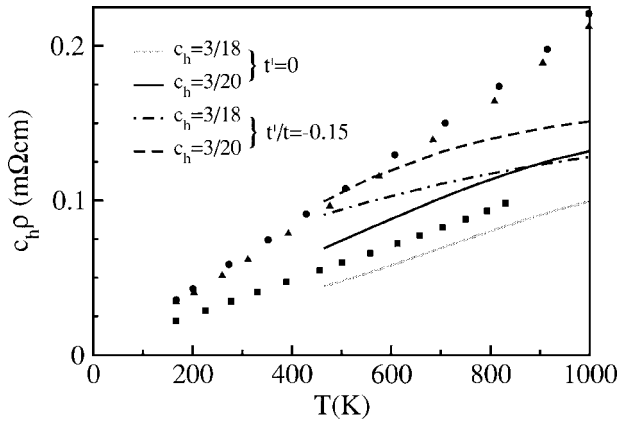


FIG. 5. Normalized resistivity $c_h\rho(T)$ at intermediate doping for $t'/t=0$ and $t'/t=-0.15$, compared with the experimental data for LSCO. Squares denote results for $x=0.15$ (Ref. 3), while circles and triangles are for $x=0.15, 0.18$ (Ref. 8), respectively.

where along the nodal direction²⁸ as well as in other directions²⁹ $\gamma \sim 0.7$ was obtained.

For comparison with the numerical result at the lowest $T/t=0.1$, we display in Fig. 4 $C(\omega)$ following from Eq. (11) with $\gamma=1.2$ and $\xi=\pi$. The qualitative behavior is satisfying, with a visible deviation only at low $\omega < T$. This indicates that anomalous $C(\omega)$ as well as the power law $\sigma(\omega) \propto \omega^{-\nu}$ with $\nu < 1$ can be qualitatively described with the assumption that the quasiparticle damping is of the MFL form with large $\gamma > 0.3$. Still, the description with the simple Eq. (11) cannot quantitatively account for the whole region $(\omega, T) < \omega_c$.

Let us discuss the quantitative comparison of our results for $\rho(T) = c/\sigma(\omega=0, T)$ (we use $c=6.6 \text{ \AA}$) with the experiments at intermediate doping. In Fig. 5 we compare experimental results for the normalized resistivity $c_h\rho$ of LSCO for $x=0.15, 0.18$ (Refs. 3 and 8) with corresponding FTLM results for $N_h=3$ in systems with $N=18, 20$ sites in the case of $t'/t=0$ and $t'/t=-0.15$, respectively. Results for $t'/t=0$ are well consistent with the linear $\rho \propto T$ law in the T regime of experimental relevance. It is characteristic that $t'/t=-0.15$ results reveal somewhat larger ρ at lower T while also the presumed linearity is reached at lower $T < 1000$ K. Taking into account the variation of different experimental data the quantitative agreement is satisfying although we allow for the possibility that our model results underestimate ρ .

IV. LOW-DOPING REGIME

In previous numerical studies of $\sigma(\omega, T)$ results for the low-doping regime^{8,5,16} were less conclusive. The reasons were the following: (a) T_{fs} increases as $c_h \rightarrow 0$. So even $T_{fs} \sim 0.15t$ was unreachable in the systems available with the FTLM a decade ago. (b) At the lowest doping, i.e., for the case of a single hole $N_h=1$, there is a significant nondissipative contribution $D_c \neq 0$ at $T \sim T_{fs}$. This indicates that the effective scattering length L_s might become larger than the system size \sqrt{N} . In addition, D_c is varying quite uncontrollably between different system sizes when the FTLM is performed with a fixed BC. In fact, as shown in Fig. 1 in several

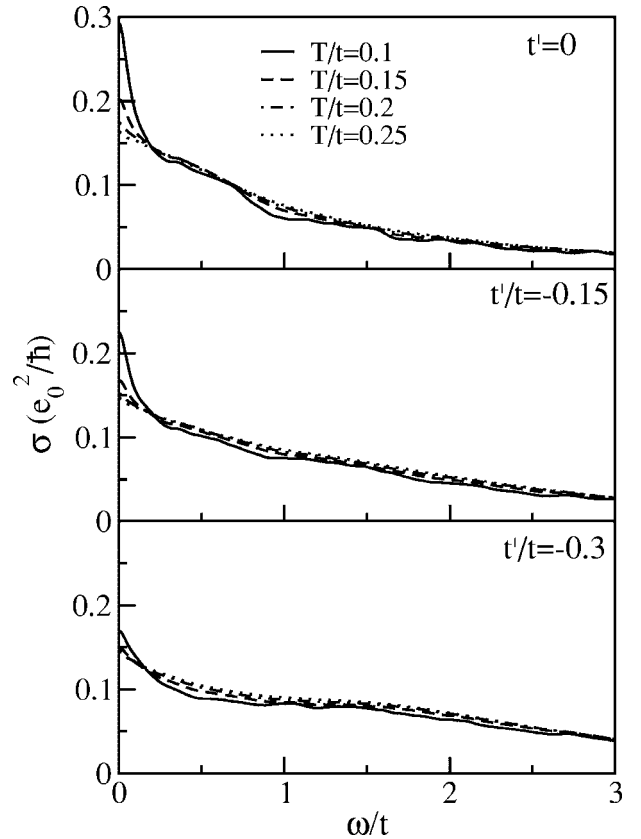


FIG. 6. 2D $\sigma(\omega)$ for underdoped $c_h=2/20$, at different T/t and t'/t .

cases one gets unphysical $D_c < 0$. (c) Systematic experimental studies of $\rho(T)$ and $\sigma(\omega)$ in cuprates at low doping have become available more recently.

The TBC averaging substantially improves the FTLM results for $\sigma(\omega)$, as seen in Fig. 1. They are much less system-size dependent even in the presence of a finite $D_c > 0$. First the results for planar $\sigma(\omega)$ in the underdoped case are presented in Fig. 6. We note that the behavior is generally very similar to the one at intermediate doping in Fig. 2. Still, there appears to be already some build-up of a shoulder at, e.g., $\omega \sim 0.5t$ for $t'/t=0$, as a precursor of the mid-IR scale, hence $\sigma(\omega)$ cannot be well described by a power law $\sigma \propto \omega^{-\nu}$ any more. Results for $c_h=0.1$ can be considered as a crossover to substantially different behavior in the low-doping regime which we discuss further.

In Fig. 7 we present results for $\sigma(\omega)$, as obtained for the largest system with $N=26$ sites and a single hole $N_h=1$. Very similar results were obtained also for $N_h=1$ in systems with $N=18, 20$ sites. The behavior of $\sigma(\omega)$ is clearly different from the one belonging to the optimum doping in Fig. 2. The main difference comes from the emergence of a shoulder at ω^* which further depends on t' . While $\omega^* \sim 0.5t$ at $t'/t=0$, it increases to $\omega^* \sim t$ for $t'/t=-0.3t$. The shoulder starts to build up in $\sigma(\omega)$ for $T < J$ which is a quite clear indication that the observed effect is related to the onset of short-range AFM correlations, confirming the relevance of the string picture of the incoherent hole motion.¹⁸ Lowering $T < J$ we are in a regime of nearly constant $\sigma(\omega < \omega^*)$ which at the same time

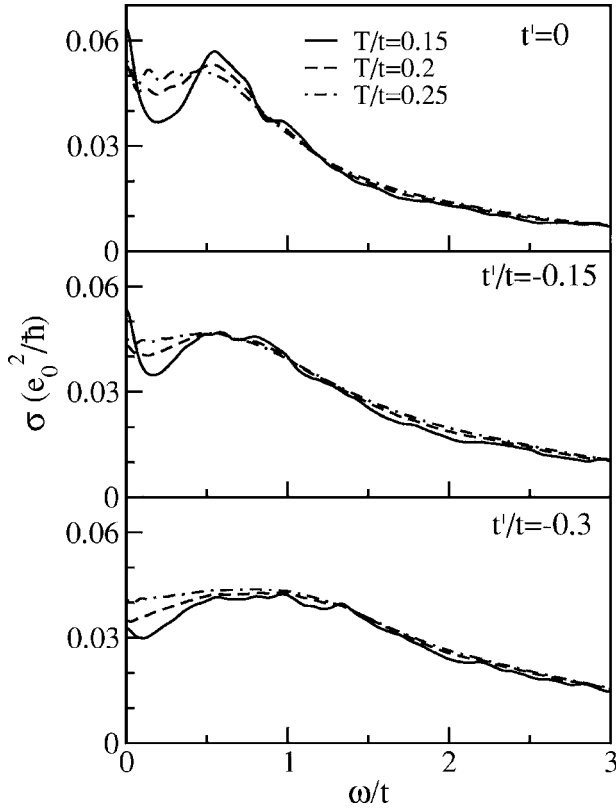


FIG. 7. 2D $\sigma(\omega)$ for low doping, calculated for $c_h=1/26$ at different T/t and t'/t .

induces the flattening or the saturation of $\rho(T)$. It should be noted that our shoulder can plausibly be related to the mid-IR resonance in cuprates,^{5,15,16} in fact the position of both is even quantitatively well in agreement. At the same time a dip in $\sigma(\omega)$ has also been observed in recent experiments in LSCO at low doping $x=0.08$ and above the crossover temperature $T > T^* \sim 500$ K,¹⁵ as well as in YBCO.¹⁶

At decreasing $T < T^* < J$ our results indicate the onset of a nondissipative contribution $D_c(T) > 0$. Calculated $D_c(T)$ are surprisingly consistent for different systems $N=18, 20, 26$, as presented in Fig. 8. Plausibly one expects that in a large enough system additional scattering channels would lead to the broadening of the $\omega=0$ peak. Nevertheless its weight should not change considerably and also its width should remain at least narrower than the pseudogap scale ω^* . Quite abrupt onset of $D_c > 0$ at $T^* \sim 0.15t \sim 600$ K is quite consistent with the experimentally observed scale T^* at low doping, identified as the kink in $\rho(T)$.^{3,8} To evaluate proper $\rho(T < T^*)$ we are missing the scattering mechanism within our small systems. For convenience we evaluate $\rho(T < T^*)$ by using spectra broadening ϵ as elsewhere in our analysis.

Let us continue with the results for the normalized 2D resistivity $c_h\rho$ presented in Fig. 9 in a large range of temperatures $T < t$ and for a wider regime of doping up to the optimum doping $c_h=0.15$. For large $T > 0.5t$ all curves merge on the trivial linear dependence $d\rho/dT = \zeta\rho_0 k_B / c_h t$ with $\zeta \sim 0.4$, as follows, e.g., from the high- T expansion for $\rho(T)$.^{10,11} For the intermediate doping there appears a steady crossover at $T \sim 0.25t$ to the low- T linear law, as discussed in

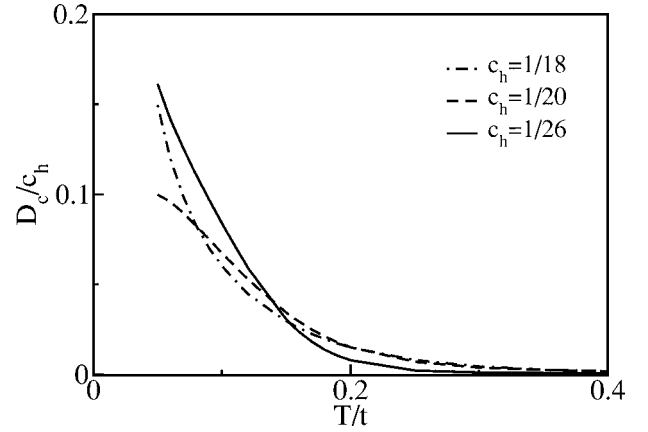


FIG. 8. Normalized charge stiffness D_c/c_h as calculated for $N_h=1$ and $N=18, 20, 26$ in the case of $t'=0$.

Sec. III. On the other hand, low-doping results reveal quite evidently a pseudosaturation of $\rho(T)$ within the T window $T^* < T < 0.5t$, closely related to the appearance of a flat and T independent $\sigma(\omega)$ in this regime. We can compare our 2D saturation value ρ_{sat} with the estimate in Refs. 13 and 14, obtained by assuming $\sigma(\omega < W) \sim \text{const}$ with W being a typical bandwidth. Since $\langle H_{\text{kin}} \rangle / N \sim -3.4tc_h(1-c_h)$ for 2D t - J model¹³ one gets from Eq. (6) at low doping $c_h \rightarrow 0$,

$$c_h \rho_{\text{sat}} \sim 0.37 \frac{W}{t} \rho_0 \sim 0.75 \rho_0, \quad (12)$$

assuming an effective width of $\sigma(\omega)$ spectra $W/t \sim 2$ as estimated from Fig. 7, and $\rho_0 = \hbar / e_0^2$ denotes the universal sheet resistivity. Our saturation value in Fig. 9 is well in agreement with the one following from Eq. (12).

Finally, we compare in Fig. 10 our results for $c_h\rho(T)$ at $t'=0$ with the experimental values for LSCO at low doping.^{3,8} First we note that the calculated values for $c_h\rho(T)$ in the low doping regime are larger compared to those at intermediate doping in Fig. 5 as observed in experiments. In the same way, it follows from Fig. 10 that $c_h\rho(T)$ is larger for $c_h=0.05$ than for $c_h=0.1$. Comparing our results for the low-

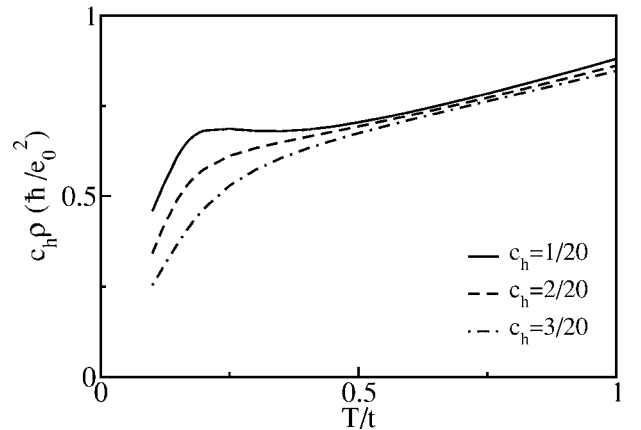


FIG. 9. Normalized 2D resistivity $c_h\rho$ vs T/t for different c_h and $t'=0$.

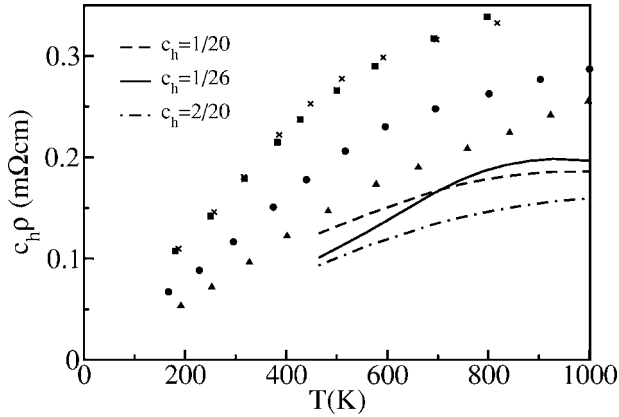


FIG. 10. Normalized resistivity $c_h \rho(T)$ at low doping for $t' = 0$ compared to experimental results for LSCO, $x = 0.04, 0.07$, crosses and squares (Ref. 3), and $x = 0.04, 0.08$, circles and triangles (Ref. 8), respectively.

est doping $c_h = 1/20, 1/26$ we can observe the behavior with a kink at $T \sim T^*$ similar to experiments. The values themselves are somewhat lower than those obtained by Ando *et al.*,⁸ and within a factor of 2 to previous data.³

V. CONCLUSIONS

Let us summarize and discuss our results for the optical conductivity $\sigma(\omega)$ and the dc resistivity $\rho(T)$ within the extended t - J model. The TBC averaging method, used in our studies, provides a clear improvement of the FTLM exact-diagonalization studies of small systems. In particular, the advantage is evident in the low-doping regime, which is one of the central points in our analysis.

Our study confirms that the transport properties substantially differ between the low-doping regime $c_h < 0.1$ and the intermediate doping, in our case $c_h \sim 0.15$. With respect to the NNN hopping t' , our results indicate that the transport quantities are not much sensitive to its value, at least for $T > T_{fs}$ which we are able to study numerically. General trend is that $t' < 0$, as appropriate for hole-doped cuprates, slightly increases $\rho(T)$ as well as the shoulder (mid-IR) scale at low doping. At the same time, the characteristic behavior at intermediate doping moves with $t' < 0$ towards the properties at lower doping. In particular, properties at $t' = 0$ and $t'/t = -0.15$ are qualitatively similar, while $t'/t = -0.3$ already exhibits more pronounced deviation even at intermediate doping.

In this paper we present results for $J/t = 0.3$ only, as believed to be the best parameter choice for cuprates. Still, additional results obtained for $J/t = 0.4$ (not shown here) reveal that both $\sigma(\omega)$ and $\rho(T)$ do not change appreciably as far as we are dealing with the strong correlation regime $J < t$.

At intermediate doping $\sigma(\omega)$ is well consistent with the anomalous scaling described within the MFL scenario. The overall behavior is close to the universal form, Eq. (7), with $C(\omega) = C_0$ in a wide range $\omega < \omega_c \sim 2t$ and $T < J$. On the other hand, we can establish also deviations from the above simple form, in particular $C(\omega)$ is an increasing function of

ω . At $\omega > T$ the scaling is thus consistent with the power law $\sigma \propto \omega^{-\nu}$ with $\nu < 1$, in particular $\nu \sim 0.65$ for $t' = 0$ very close to recent experimental result for BSCCO,² although one would expect better agreement with $t' < 0$ results in the latter cuprates.

The anomalous behavior of $\sigma(\omega)$ and $C(\omega)$ can be partly understood in terms of a simple representation of electron spectral functions, Eq. (11), where the quasiparticle damping $\Gamma = \gamma(|\omega| + \xi T)$ is of the MFL form with large $\gamma > 0.3$. It should be also noted that $C(\omega)$, Eq. (11), leads in general to an analytical dependence at small ω , i.e., $T\sigma(\omega \rightarrow 0) \sim B + A(\omega/T)^2$,²⁷ in contrast to the simple $C(\omega) = C_0$ assumption. Still, we find that the same input for γ which can describe the high- ω behavior cannot quantitatively account for experimentally observed $\omega/T \rightarrow 0$.²

The origin of the anomalous MFL-like behavior of $\sigma(\omega)$ has not been clarified yet. The scaling range $\omega < 2t$ is surprisingly broad, since one would expect that it might be also determined by J . On the other hand, the behavior qualitatively changes for $T > J$.^{10,12} This is another sign, that we are dealing with an unusual frustrated fermionic system and possibly not with the quantum phase transition² which should possess only a single scale in the (ω, T) diagram.

At low doping $c_h < 0.1$ the behavior changes qualitatively. $\sigma(\omega)$ exhibits a shoulder at ω^* and flat region or a weak dip for $\omega < \omega^*$, as found also in recent measurements in LSCO (Ref. 15) and YBCO.¹⁶ The shoulder is clearly related to the mid-IR peak found in experiments, whereby we find $\omega^* > 2J$ being in a reasonable quantitative agreement. The shoulder sets in for $T < J$ and is plausibly related to the onset of short-range AFM correlations hence this confirms the magnetic origin of the mid-IR resonance and its spin-string interpretation.^{17,18} Another manifestation of the same phenomenon is the saturation of $\rho(T)$ in the temperature window $T^* < T < J$ which is in agreement with experiments in cuprates.¹⁴

For $T < T^*$ we observe the onset of a coherent transport in our small systems, which shows up in a rather abrupt increase of the charge stiffness $D_c(T)$. The appearance of $D_c(T) > 0$ means that the scattering length $L_s(T)$ becomes larger than the system size \sqrt{N} . In this connection, it is quite puzzling to explain why $L_s(T)$ is larger in the low doping regime than at intermediate doping. That is, we find $D_c \sim 0$ down to $T \sim T_{fs}$ at $c_h = 0.15$, whereas evidently we get $D_c > 0$ at the same T in the low-doping regime. This apparent contradiction is, however, consistent with recent experimental confirmation of a quite coherent transport at low doping for $T < T^*$ and the concept of a nodal metal.^{8,16}

While qualitative behavior of $\rho(T)$ is well in agreement with experiments, let us finally comment on the quantitative comparison. At intermediate doping the normalized resistivity $c_h \rho(T)$ lies tolerably within the range of existing experimental values for LSCO, taking into account also some variation between different published results. At low doping our results seem to underestimate somewhat $\rho(T)$. Still, the discrepancy (depending again on different experimental data) is at most of a factor of 2. Whether this rather modest disagreement is an indication of the possible relevant role of degrees of freedom outside the t - J model, remains an open question.

ACKNOWLEDGMENTS

We acknowledge the discussion with O. Gunnarsson, and the use of unpublished data by Y. Ando and co-workers. This

work was funded by the Ministry of Higher Education, Science and Technology of Slovenia under Grant No. PI-0044. One author (P.P.) also acknowledges the support of the Alexander von Humboldt Foundation.

-
- ¹C. M. Varma, P. B. Littlewood, S. Schmitt-Rink, E. Abrahams, and A. E. Ruckenstein, *Phys. Rev. Lett.* **63**, 1996 (1989).
- ²D. van der Marel, H. J. A. Molegraaf, J. Zaanen, Z. Nussinov, F. Carbone, A. Damascelli, H. Eisaki, M. Greven, P. H. Kes, and M. Li, *Nature (London)* **425**, 271 (2003).
- ³H. Takagi, B. Batlogg, H. L. Kao, J. Kwo, R. J. Cava, J. J. Krajewski, and W. F. Peck, Jr., *Phys. Rev. Lett.* **69**, 2975 (1992).
- ⁴Y. Ando, S. Komiya, K. Segawa, S. Ono, and Y. Kurita, *Phys. Rev. Lett.* **93**, 267001 (2004).
- ⁵S. Uchida, T. Ido, H. Takagi, T. Arima, Y. Tokura, and S. Tajima, *Phys. Rev. B* **43**, 7942 (1991).
- ⁶A. V. Puchkov, D. N. Basov, and T. Timusk, *J. Phys.: Condens. Matter* **8**, 10049 (1996).
- ⁷For a review see, T. Timusk, *Solid State Commun.* **127**, 337 (2003).
- ⁸Y. Ando, A. N. Lavrov, S. Komiya, K. Segawa, and X. F. Sun, *Phys. Rev. Lett.* **87**, 017001 (2001); S. Ono, S. Komiya, and Y. Ando (unpublished).
- ⁹J. Jaklič and P. Prelovšek, *Phys. Rev. B* **49**, 5065 (1994).
- ¹⁰For a review see, J. Jaklič and P. Prelovšek, *Adv. Phys.* **49**, 1 (2000).
- ¹¹J. Jaklič and P. Prelovšek, *Phys. Rev. B* **50**, 7129 (1994); **52**, 6903 (1995).
- ¹²J. Jaklič and P. Prelovšek, *Phys. Rev. Lett.* **75**, 1340 (1995).
- ¹³M. Calandra and O. Gunnarsson, *Europhys. Lett.* **61**, 88 (2003).
- ¹⁴For a review see, O. Gunnarsson, M. Calandra, and J. E. Han, *Rev. Mod. Phys.* **75**, 1085 (2003).
- ¹⁵K. Takenaka, R. Shiozaki, S. Okuyama, J. Nohara, A. Osuka, Y. Takayanagi, and S. Sugai, *Phys. Rev. B* **65**, 092405 (2002).
- ¹⁶Y. S. Lee, K. Segawa, Z. Q. Li, W. J. Padilla, M. Dumm, S. V. Dordevic, C. C. Homes, Y. Ando, and D. N. Basov (unpublished).
- ¹⁷I. Sega and P. Prelovšek, *Phys. Rev. B* **42**, 892 (1990).
- ¹⁸For a review see, E. Dagotto, *Rev. Mod. Phys.* **66**, 763 (1994).
- ¹⁹T. Tohyama and S. Maekawa, *Phys. Rev. B* **64**, 212505 (2001).
- ²⁰For a review see, A. Damascelli, Z. Hussain, and Z.-X. Shen, *Rev. Mod. Phys.* **75**, 473 (2003).
- ²¹R. Raimondi, J. H. Jefferson, and L. F. Feiner, *Phys. Rev. B* **53**, 8774 (1996).
- ²²E. Pavarini, I. Dasgupta, T. Saha-Dasgupta, O. Jepsen, and O. K. Andersen, *Phys. Rev. Lett.* **87**, 047003 (2001).
- ²³D. Poilblanc, *Phys. Rev. B* **44**, 9562 (1991).
- ²⁴J. Bonča and P. Prelovšek, *Phys. Rev. B* **67**, 085103 (2003).
- ²⁵P. F. Maldague, *Phys. Rev. B* **16**, 2437 (1977).
- ²⁶W. Kohn, *Phys. Rev.* **133**, 171 (1964).
- ²⁷P. Prelovšek, *Europhys. Lett.* **53**, 228 (2001).
- ²⁸T. Valla, A. V. Fedorov, P. D. Johnson, B. O. Wells, S. L. Hulbert, Q. Li, G. D. Gu, and N. Koshizuka, *Science* **285**, 2110 (1999).
- ²⁹A. Kaminski, H. M. Fretwell, M. R. Norman, M. Randeria, S. Rosenkranz, U. Chatterjee, J. C. Campuzano, J. Mesot, T. Sato, T. Takahashi, T. Terashima, M. Takano, K. Kadowaki, Z. Z. Li, and H. Raffy, *Phys. Rev. B* **71**, 014517 (2005).